



Published in final edited form as:

Breast Cancer Res Treat. 2020 September ; 183(2): 403–410. doi:10.1007/s10549-020-05780-6.

The Shape of Breast Cancer

Brook K. Byrd¹, Venkataramanan Krishnaswamy, Ph.D.², Jiang Gui, Ph.D.⁵, Timothy Rooney, MD³, Rebecca Zuurbier, MD³, Kari Rosenkranz, MD⁴, Keith Paulsen, Ph.D.¹, Richard J. Barth Jr., MD⁴

¹Thayer School of Engineering, Dartmouth College, Hanover, NH

²CairnSurgical, Inc., Lebanon, NH

³Department of Radiology, Dartmouth-Hitchcock Medical Center, Lebanon, NH

⁴Department of Surgery, Dartmouth-Hitchcock Medical Center, Lebanon, NH

⁵Dartmouth Geisel School of Medicine, Hanover, NH

Abstract

Purpose: Little is known about the three-dimensional shape of breast cancer. Implicit to approaches that localize the center of the tumor for breast conserving surgery (BCS) of non-palpable cancers is the assumption that breast cancers are spherical about a central point, which may not be accurate.

Methods: Pre-operative supine breast MRI images were obtained of 83 breast cancer patients undergoing partial mastectomy using supine MRI guided resection techniques. Three-dimensional (3D) tumor models were derived after radiologists outlined tumor edges on successive MRI slices. Ideal resection volumes were determined by adding 1 cm in every dimension to the actual tumor volume. Geometrically defined parameters were used to define tumor shapes and associations between clinical variables and shapes were examined.

Terms of use and reuse: academic research for non-commercial purposes, see here for full terms. <https://www.springer.com/aam-terms-v1>

Corresponding Author: Richard J. Barth Jr. MD, Section of General Surgery, Dartmouth-Hitchcock Medical Center, 1 Medical Center Drive, Lebanon, NH 03756, Richard.J.Barth.Jr@hitchcock.org, +01-603-650-9479.

Compliance with Ethical Standards

Ethical Approval : All procedures performed in studies involving human participants were in accordance with the ethical standards of the Dartmouth Committee for the Protection of Human Subjects and with the 1964 Helsinki declaration and its later amendments.

Informed consent : Informed consent was obtained from all individual participants included in the study.

Data Availability Statement

The datasets generated during and/or analysed during the current study are available from the corresponding author on reasonable request.

Conflict of Interest: Drs. Barth, Krishnaswamy and Paulsen have ownership interest in CairnSurgical Inc. This work was supported by National Institutes of Health/National Cancer Institute(NIH/NCI) Grant R21CA182956 to RJB and 2R44CA210810–02 to CairnSurgical Inc. A relevant US patent 15/735,907 has been exclusively licensed to CairnSurgical, Inc. Brook Byrd, Jiang Gui, Timothy Rooney, Rebecca Zuurbier, and Kari Rosenkranz have no conflicts of interest to declare.

Publisher's Disclaimer: This Author Accepted Manuscript is a PDF file of an unedited peer-reviewed manuscript that has been accepted for publication but has not been copyedited or corrected. The official version of record that is published in the journal is kept up to date and so may therefore differ from this version.

Results: Seventy five patients had invasive cancer. Breast cancers were categorized into 4 tumor shapes: 34% of tumors were discoidal, 29% segmental, 19% spherical and 18% irregular. If hypothetical spherical excisions were performed, nonspherical cases would excise 143% more tissue than the ideal resection volume. When the 3D shape of each tumor was provided to the surgeon during MR-guided BCS, the percentage of tissue overexcised in non-spherical cases was significantly less (143% vs. 66% , $p < 0.001$).

Conclusions: Information obtained from a supine MRI can be used to generate 3D tumor models and rapidly classify breast tumor shapes. The vast majority of invasive cancers and DCIS are not spherical. Knowledge of tumor shape may allow surgeons to excise breast cancer more precisely.

Keywords

MRI; breast cancer; Breast shape; supine; breast conserving surgery; lumpectomy

1. Introduction

Successful breast-conserving surgery (BCS) of patients without palpable neoplasms relies on image-guidance tools and the skills of surgeons and has the goal of completely removing the tumor with appropriate surgical margins. Even with an influx of novel surgical guidance technologies, the positive margin rate in BCS, which ranges from 15–30%, remains an issue yet to be solved completely by any one technology [1–5]. If a positive margin is identified, an additional re-excision surgery is necessary which increases the emotional burden and financial cost to the patient and healthcare system.

The standard of care for localizing non-palpable breast cancer and DCIS is wire localization. Point-based technologies that utilize radioactive or magnetic seeds or reflectors are increasing in popularity because they may facilitate surgical scheduling [4]. Although occasionally used to bracket extensive areas of neoplasia, in most cases both wire localization and point-based technologies are intended to identify the center of the tumor for the surgeon. These methods do not inform the surgeon about the volumetric shape or three-dimensional extents of the cancer. Led by point-based guidance, surgeons may assume that breast cancer is spherical and design their excision accordingly. Furthermore, presurgical MR planning images offer only a limited number of 2D views which hinders a surgeon's ability to visualize the 3D shape of the target excision in each BCS case.

In comparison to breast MRI done in the prone position, breast MRI done in the supine position gives the surgeon an image of the cancer and its position in the breast that corresponds to the shape and relative position of the tumor when the patient is supine on the operating room table. Herein, we characterize and explore trends in the 3D shapes of tumors from a group of breast cancer patients who had supine MRIs and underwent BCS utilizing technologies that relied on supine MRI data to guide BCS. We also evaluated the potential effect of tumor shape on BCS excision volumes by: 1) comparing a hypothetical spherical excision to the MRI-defined tumor volume and 2) comparing actual resection volumes obtained using MRI-guided surgery with the MRI-defined tumor volume.

2. Methods

Patients for this study were entered on one of two prospective experimental studies of technologies used for supine MRI guided surgery (2,6). Both studies were approved by the Dartmouth Committee for the Protection of Human Subjects. Sixty seven patients were treated on “A Randomized Prospective Trial of Supine MRI Guided vs. Wire Localization Lumpectomy for Breast Cancer”, [ClinicalTrials.gov #NCT01929395](https://clinicaltrials.gov/ct2/show/study/NCT01929395) [2]. All of these patients had non-palpable breast cancer. They underwent BCS by surgeons who had access in the OR to a virtual 3D model of the cancer derived from supine MRI images and used an intra-operative tracking system to outline the projected tumor edges on the skin surface. The 3D model of the cancer in the breast informed the surgeon of the shortest distance from the tumor to the skin and from the tumor to the chest wall and allowed the surgeon to see which part of the tumor was closest to the skin or chest wall. The surgeon used this information and the tumor outline on the skin surface to do the lumpectomy; no wires were placed (as more fully described elsewhere [2]). The remainder of the patients (16) had palpable breast cancer that was excised by surgeons who had access in the OR to the same virtual 3D model of the cancer derived from supine MRI and used a 3D printed bra-like form (the Breast Cancer Locator, BCL) to identify projected tumor edges on the skin surface and mark the tumor edges within the breast parenchyma (6). The surgeon placed the BCL on the patient’s breast prior to surgery and used it to mark the projected tumor edges on the skin surface and to inject blue dye into the breast to define the tumor edges. Surgery was done utilizing these cues and no wires, as more fully described elsewhere (6). These patients were treated on The Pilot BCL Study, [ClinicalTrials.gov # NCT02550210](https://clinicaltrials.gov/ct2/show/study/NCT02550210) [6].

During both of these studies, patients underwent contrast-enhanced T1-weighted breast MRI in the supine position on either a Phillips 3T MRI scanner (Phillips Healthcare, Andover, MA) with circular coils, or a Siemens 1.5 T scanner (MAGNETOM Area, Siemens Healthineers, Malvern, PA) with a rectangular flex coil. A soft pad was placed on the sternum to support the rectangular flex coil. The pad was designed with cut-outs for each breast, which minimized breast deformation. Patients were positioned in the scanner with their ipsilateral arm parallel to their body. A pre-injection T1-weighted ultrafast gradient echo sequence was acquired to define the breast volume and tissue structures while a post-injection T1-weighted turbo gradient echo volume acquisition with fat saturation was used to determine tumor location and shape. A radiologist outlined the tumor edges on contiguous axial MRI slices acquired with the patient positioned in the surgical (supine) position. A 3D virtual model of the tumor, breast surface and chest wall was constructed from the MRI data based on segmented models obtained with 3D Slicer (Version 4.3.1, www.slicer.org) software [7]. It takes a radiologist approximately 10 minutes to outline the tumor edges on the supine MRI images and then approximately 1 minute for the 3D virtual tumor model to be created. One centimeter margins were expanded in all directions about the segmented tumor shape to generate ‘ideal’ tumor excision models.

Geometric Definitions of Tumor Shapes

We defined four tumor shape categories based on their geometric characteristics- spherical, segmental, discoidal and irregular. To describe the spherical or nonspherical nature of each tumor shape, a sphericity metric (previously defined [8]) was calculated (Eq. 1) as-

$$\Psi = \frac{1}{\pi^{\frac{1}{3}}(6V_{tumor})^{\frac{2}{3}}}/SA_{tumor} \quad (1)$$

where V represented the computed tumor model volume and SA denoted its corresponding surface area. A secondary metric, isocentricity was also computed and utilized for shape categorization. This measure (Eq. 2), compared the maximal (d_{max}) and minimal (d_{min}) tumor extents from the center of the tumor to evaluate tumor compactness (See Figure 1(a)).

$$\Psi = \frac{1}{\pi^{\frac{1}{3}}(6V_{tumor})^{\frac{2}{3}}}/SA_{tumor} \quad (2)$$

A perfect sphere has a sphericity value (Ψ) of 1 and an isocentricity value of 0. We defined tumors with sphericity values (Ψ) above 0.75 or an isocentricity value below 1 to be spherical.

Tumor diameters along three orthogonal principle axes were measured by fitting each tumor shape to the smallest possible ellipsoid shape found through singular value decomposition. As shown in Fig. 1(b), the three primary axes of the fitted ellipsoids, for each respective shape, were used to differentiate between segmental, discoidal, and irregular shapes. Long and tubular shapes were classified as segmental- defined by one axis of the fitted ellipsoid being 50% longer than the other two ellipsoid axes. Flat and disk-like shapes were classified as discoidal -defined by one axis being 50% shorter than the other two primary axes of the fitted ellipsoid. Tumors that did not fit the geometric criteria for spherical, discoidal, or segmental were defined as “irregular”. Post-classification, all shapes were visually surveyed to ensure accuracy and credibility of the classification scheme.

We tested relationships between the shape of tumors and clinical variables. For discrete clinical variables, such as cancer type and positive margin status, chi-squared tests were performed to identify possible associations. Margins were considered positive based on the Consensus definitions from the Society for Surgical Oncology (9,10). For clinical measurements, such as tumor volume and age, ANOVA tests were performed to identify significant differences in average measurements across shape categories. If a significant difference was found amongst shape categories ($p < 0.05$) Tukey’s *post hoc* test was performed to identify which two categories differed significantly.

To evaluate effects of tumor shape on the BCS target excision volume in each case, we fit the smallest possible sphere to each tumor model with 1 cm margins and measured the excess tissue volume excised by such a hypothetical spherical excision (See Fig. 1(c)). This hypothetical excision was compared to ‘ideal’ resection volumes, which were determined by expanding the tumor model surface 1 cm in each dimension. Lastly, *actual* tumor resection volumes were also measured by water displacement at the time of surgery for all cases. Comparisons were made between the hypothetical spherical and ‘ideal’ excision volume and

between the actual excision and ‘ideal’ excision volumes for each patient in the trials using paired T-tests. The percentage of volume overexcised was calculated as (actual or hypothetical volume excised – ideal volume)/ideal volume X 100.

3. Results

Breast cancers were categorized into 4 tumor shapes: 34% of tumors were discoidal, 29% segmental, 19% spherical and 18% irregular. Examples of 5 tumors from each of the shape categories are shown in Figure 2. Examples of the 3D reconstructed tumor shapes compared to the 2D images of these tumors on prone and supine MRI are shown in Figure 3. These comparisons highlight the additional information provided to the surgeon by the 3D tumor shape when compared to one cross-sectional slice of MRI data.

Table 1 displays the relationship between pathologic findings and tumor shape. None of 8 DCIS tumors were spherical; half were discoidal and half were segmental. Of 64 invasive ductal cancers, 31% were discoidal, 25% segmental, 23% spherical and 20% irregular. Only 1 of 11 (9%) infiltrating lobular cancers was spherical; 36% were discoidal, 25% segmental and 13% irregular. No significant difference was evident in the shape of infiltrating ductal vs. infiltrating lobular carcinomas.

As shown in Table 2, the mean patient age was 64 years. Most of the cancers were non-palpable (67/83, 81%); 16/83 (19%) were palpable. The mean pathologic tumor diameter was 1.94 cm. Seventy five percent of the tumors were estrogen receptor positive. Ten of 75 invasive cancers (13%) were node positive. No significant correlation was found between cancer shape and patient age, estrogen receptor positivity, Her-2 status, mean pathologic tumor diameter or the presence of nodal metastases (Table 2). Of note, there was an association between largest tumor diameter on MRI and tumor shape, with discoid tumors having the largest diameter ($d_{max} = 2.56$ cm) and spherical tumors having the smallest diameter ($d_{max} = 1.59$ cm) ($p = 0.01$).

Breast conserving surgery performed with knowledge of the 3D tumor location and shape and supine MRI guidance resulted in positive margins in 7/83 (8%) of cases (5/75 patients with invasive cancer and 2/8 patients with DCIS had positive margins). No significant difference was found in the positive margin rate according to tumor shape: spherical 2/16 (12%), discoidal 0/28 (0%), segmental 4/24 (17%), irregular 1/15 (7%), $p = 0.17$.

We evaluated the potential effect of tumor shape on BCS excision volume by fitting the smallest possible sphere to the ideal resection tumor shape and measuring the excess tissue volume excised by a hypothetical spherical excision when compared to the ideal resection volume. As seen in Figure 4(a), the overexcised volume in hypothetical spherical excisions was significantly higher for the discoidal (172%), segmental (114%), and irregular (139%) tumors than for the sphere-shaped tumors (50%) (sphere vs. disk, $p < 0.001$; sphere vs. segmental, $p < 0.001$; sphere vs. irregular, $p = 0.003$). When surgeons performed MR-guided BCS, the percent excess volume of tissue actually removed was markedly less than the hypothetical spherical excision volume in the discoidal (66% vs. 172%), segmental (62% vs. 113%), and irregular tumors (75% vs. 139%)(Fig. 4b). This difference was statistically

significant for discoidal tumors ($p < 0.001$) and marginally significant for segmental ($p = 0.06$) and irregular tumors ($p = 0.08$). When all non-spherical cases were considered together, the over-excised volume was significantly less when the actual volume excised in MR guided BCS cases was compared to the hypothetical spherical excision volume (66% vs. 143%, $p < 0.001$).

We also compared the maximal tumor diameter (MTD), as computed from the 3D MRI models, with the MTD described in the prone MRI radiology report. The mean MTD of the 3D tumor models (3.9 cm, SD = 1.7 cm) was significantly greater than the mean MTDs reported by the Radiologists (2.5 cm, SD = 1.4) ($p < 0.0001$). The MTD computed from the 3D model was greater than the MTD in the prone MRI report in 80% of patients, and was at least 1 cm greater than the MTD in the MRI report in 61% of cases.

4. Discussion

This paper is the first, to our knowledge, to describe breast cancer shapes based on supine MRI data. By applying geometric formulas to 3D tumor reconstructions, we classified 83 breast cancers into 4 distinct shapes: spherical, discoidal, segmental and irregular. Overall, only 19% of breast cancers were spherical; the most common shapes were discoidal (34%) and segmental (29%). Spherical tumors were particularly uncommon in the subsets of patients with DCIS (0/8) and infiltrating lobular cancer (1/11).

Similar results were reported by Uematsu et al., who reported the shape of breast cancers in 134 patients who underwent prone MRI [11]. Their analysis of serial MRI images showed that breast cancers could be categorized into 4 shapes: 32% were oval, 26% lobulated, 26% irregular and 16% were round. Although their methodology was less quantitative than ours (for example, the authors did not create 3D models of the breast cancers, nor did they fit geometric models to segmented shapes), they also found that less than 20% of their patients had spherical (round) tumors.

Observations from a limited number of pathologic analyses also support our findings. In 1996, Wapnir et al. evaluated breast cancer shapes by measuring three perpendicular diameters of breast cancer pathology specimens [12]. They studied 165 cancers, all of which were < 2.5 cm in greatest diameter. These authors also described 4 different tumor shapes: spheres, “oblate” tumors, “prolate” tumors and irregular tumors (which had diameters with 3 different dimensions). Their “oblate” category corresponds with our discoidal shape (with two large and one smaller diameter). Their “prolate” shape corresponds with our segmental shape (with two small and one large diameter). Interestingly, only 6 of their 165 patients (4%) had cancers categorized as true spheres. Eighteen percent of patients had “oblate” (discoidal) tumors, 32% had “prolate” (segmental) tumors and 46% had irregularly shaped cancers.

In another study, Merrill et al evaluated the shape of eight breast cancers in patients who had not received neoadjuvant therapy [13]. They performed serial sectioning of tissue blocks at 100 micrometer intervals, scanned the sections and generated 3D reconstructions. They then visually picked a shape that best corresponded to the 3D reconstructions. The study

included 5 infiltrating ductal cancers, 2 infiltrating lobular carcinomas and 1 DCIS. The majority of tumors were either linear or ellipsoid in shape; only 3/8 (37%) were considered to be approximately spherical. Thus, the preponderance of evidence from studies that evaluated breast tumor shape pathologically or from MRI data indicates that the vast majority of breast cancers do not have a spherical shape.

Knowledge of the shape of breast cancer is important for performing precise breast conserving surgery. Current localization methods for non-palpable cancers attempt to identify the approximate tumor center using various techniques (eg. a wire, a radioactive seed, a magnetic chip). These localizing systems provide no further guidance regarding the location of the tumor edges; the surgeon must estimate the distance from the approximate tumor center to the tumor edge using the image defined tumor diameters in combination with assumptions about tumor shape. Even if two wires or detectors are deployed to bracket a tumor, visualizing the tumor shape from static CC and MLO mammography images is difficult. As shown in Fig 3, understanding tumor shape from a few axial and coronal MRI cross-sections is challenging, and may not capture the true extent of the disease in many instances. Therefore, in many cases, the surgeon may just assume that the tumor is spherical. This has some biologic credence; we can imagine that the cancer started as a single cell and then continued to divide and expand in all directions. However, this simplistic model ignores studies of tumor growth, a complex phenomenon influenced by the nature of the surrounding breast tissue (eg. fat vs fibrous stroma vs lobules) [14, 15].

We have now demonstrated that basing a breast conserving resection on an assumption that the tumor is spherical will result in marked overexcision of normal breast tissue. The overexcised volume was 172% of the actual tumor volume for discoidal tumors, 114% for segmental tumors and 139% for irregular tumors. In contrast, when surgery is based on a knowledge of breast cancer shape, we have shown that significantly less breast tissue was actually overexcised for non-spherical tumors (overexcised volume 66% vs 143%, $p < 0.001$). Given the well established relationship between the amount of breast tissue excised and cosmesis [16, 17] improved cosmetic outcomes are likely in patients treated with more precise BCS.

Another advantage of generating a 3D tumor model that includes tumor shape is a more accurate understanding of the maximal tumor diameter. Pathologic studies based on digitalized whole mount serial sections have shown that assessment of the entire tumor results in a significantly larger maximal tumor diameter than reported by conventional pathology in 62% of cases [18]. We have now shown that 3D modelling of tumors based on supine MRI data results in significantly greater maximal diameters, relative to values routinely described in MRI radiology reports. In fact, the maximal tumor diameter computed from the 3D model was greater than the MRI report in 80% of patients, and was at least 1 cm greater than the MRI report in 61% of cases. The concept is that by creating a 3D model, using digitalized pathologic serial sections or serial MRI images, one can identify and measure distances from one tumor edge to another that are simply not visible and able to be measured when one looks at just a small number of pathologic or MRI slices through a tumor. This finding is clinically significant, since we have shown recently that underestimation of tumor size is strongly associated with positive margins when performing

breast conserving surgery [2]. Both serial sectioning of pathology specimens and 3D modelling of consecutive supine MRI images may more accurately determine tumor size than conventional methods.

The purpose of this paper was to describe the shape of breast cancer as defined by supine MRI images and to suggest potential reasons why a better understanding of tumor shape might be clinically useful. Further research would need to be done to provide clinical and economic justification for the routine use of supine MRI in BCS. We are currently accruing patients to a multi-center randomized prospective trial comparing wire localized partial mastectomy to supine MRI guided BCS using the Breast Cancer Locator system. A cost analysis is one of the endpoints of this trial.

5. Conclusions

In summary, a gap in knowledge currently exists in understanding the 3D shape and orientation of the tumor volume within the surgical field. This study is the first to establish multi-dimensional parameters for the characterization of the shape of breast cancer based on supine MRI data. Information obtained from a supine MRI can be used to generate 3D tumor models that characterize breast tumor shapes rapidly in the surgical position. Most breast cancers and DCIS are not spherical. Knowledge of breast cancer shape may allow surgeons to excise breast cancer more precisely.

Acknowledgments

Funding: This work was supported by the National Institutes of Health and the National Cancer Institute Grant Numbers: R21CA182956 & 2R44 CA210810-0

References

1. Kaczmarek K, Wang P, Gilmore R, et al. (2019) Surgeon Re-Excision Rates after Breast Conserving Surgery: A Measure of Low-Value Care. *Journal of the American College of Surgeons* 228:504–512.e2. 10.1016/j.jamcollsurg.2018.12.043
2. Barth RJ, Krishnaswamy V, Paulsen KD, et al. (2019) A Randomized Prospective Trial of Supine MRI-Guided Versus Wire-Localized Lumpectomy for Breast Cancer. *Ann Surg Oncol*. 10.1245/s10434-019-07531-4
3. Chagpar AB, Killelea BK, Tsangaris TN, et al. (2015) A Randomized, Controlled Trial of Cavity Shave Margins in Breast Cancer. *New England Journal of Medicine* 373:503–510. 10.1056/NEJMoa1504473
4. Hayes MK (2017) Update on Preoperative Breast Localization. *Radiologic Clinics* 55:591–603. 10.1016/j.rcl.2016.12.012 [PubMed: 28411682]
5. Corsi F, Sorrentino L, Bossi D, et al. (2013) Preoperative Localization and Surgical Margins in Conservative Breast Surgery. *International Journal of Surgical Oncology* 2013:1–9. 10.1155/2013/793819
6. Barth RJ, Krishnaswamy V, Paulsen KD, et al. (2017) A Patient-Specific 3D-Printed Form Accurately Transfers Supine MRI-Derived Tumor Localization Information to Guide Breast-Conserving Surgery. *Ann Surg Oncol* 24:2950–2956. 10.1245/s10434-017-5979-z [PubMed: 28766199]
7. Fedorov A, Beichel R, Kalpathy-Cramer J, et al. (2012) 3D Slicer as an image computing platform for the Quantitative Imaging Network. *Magnetic Resonance Imaging* 30:1323–1341. 10.1016/j.mri.2012.05.001 [PubMed: 22770690]

8. Wadell H (1935) Volume, Shape, and Roundness of Quartz Particles. *The Journal of Geology* 43:250–280. 10.1086/624298
9. Moran M, Schnitt S, Giuliano A et al. Society of Surgical Oncology-American Society for Radiation Oncology consensus guideline on margins for breast-conserving surgery with whole breast radiation in stages I and II invasive breast cancer. *J Clin Onc* 2014; 32: 1507–15.
10. Morrow M, Van Zee K, Solin L et al. Society of Surgical Oncology-American Society for Radiation Oncology-American Society of Clinical Oncology consensus guideline on margins for breast conserving surgery with whole breast irradiation in ductal carcinoma in situ. *Ann Surg Oncol* 2016. 23: 3801–10. [PubMed: 27527714]
11. Uematsu T, Kasami M, Yuen S (2009) Triple-Negative Breast Cancer: Correlation between MR Imaging and Pathologic Findings. *Radiology* 250:638–647. 10.1148/radiol.2503081054 [PubMed: 19244039]
12. Wapnir IL, Wartenberg DE, Greco RS (1996) Three dimensional staging of breast cancer. *Breast Cancer Res Tr* 41:15–19. 10.1007/BF01807032
13. Merrill AL, Buckley J, Tang R, et al. (2017) A Study of the Growth Patterns of Breast Carcinoma Using 3D Reconstruction: A Pilot Study. *The Breast Journal* 23:83–89. 10.1111/tbj.12688 [PubMed: 27860134]
14. Anderson ARA, Weaver AM, Cummings PT, Quaranta V (2006) Tumor Morphology and Phenotypic Evolution Driven by Selective Pressure from the Microenvironment. *Cell* 127:905–915. 10.1016/j.cell.2006.09.042 [PubMed: 17129778]
15. Bearer EL, Lowengrub JS, Frieboes HB, et al. (2009) Multiparameter Computational Modeling of Tumor Invasion. *Cancer Res* 69:4493–4501. 10.1158/0008-5472.CAN-08-3834 [PubMed: 19366801]
16. Heil J, Breitzkreuz K, Golatta M, et al. (2012) Do Reexcisions Impair Aesthetic Outcome in Breast Conservation Surgery? Exploratory Analysis of a Prospective Cohort Study. *Ann Surg Oncol* 19:541–547. 10.1245/s10434-011-1947-1 [PubMed: 21761099]
17. Abe SE, Hill JS, Han Y, et al. (2015) Margin re-excision and local recurrence in invasive breast cancer: A cost analysis using a decision tree model. *Journal of Surgical Oncology* 112:443–448. 10.1002/jso.23990 [PubMed: 26374088]
18. Clarke GM, Holloway CMB, Zubovits JT, et al. (2019) Three-dimensional tumor visualization of invasive breast carcinomas using whole-mount serial section histopathology: implications for tumor size assessment. *Breast Cancer Res Treat* 174:669–677. 10.1007/s10549-018-05122-7 [PubMed: 30612274]

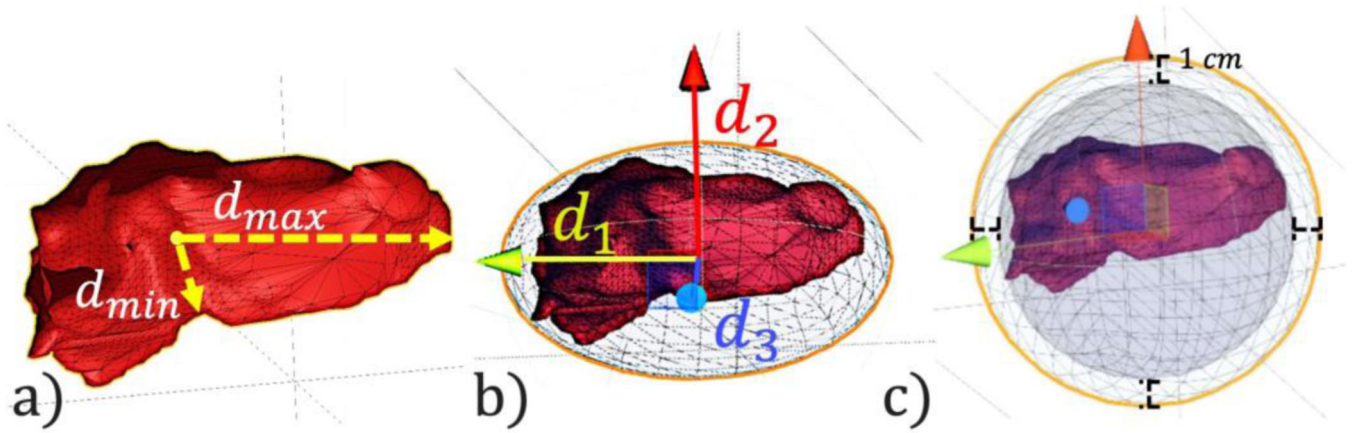


Fig. 1. (a) Maximum (d_{max}) and minimum (d_{min}) tumor extents calculated from central point of tumor. (b) Spherical excision volume with 1 cm margin on all sides. (c) Ellipsoid fit of tumor with three primary axes to characterize tumor shape

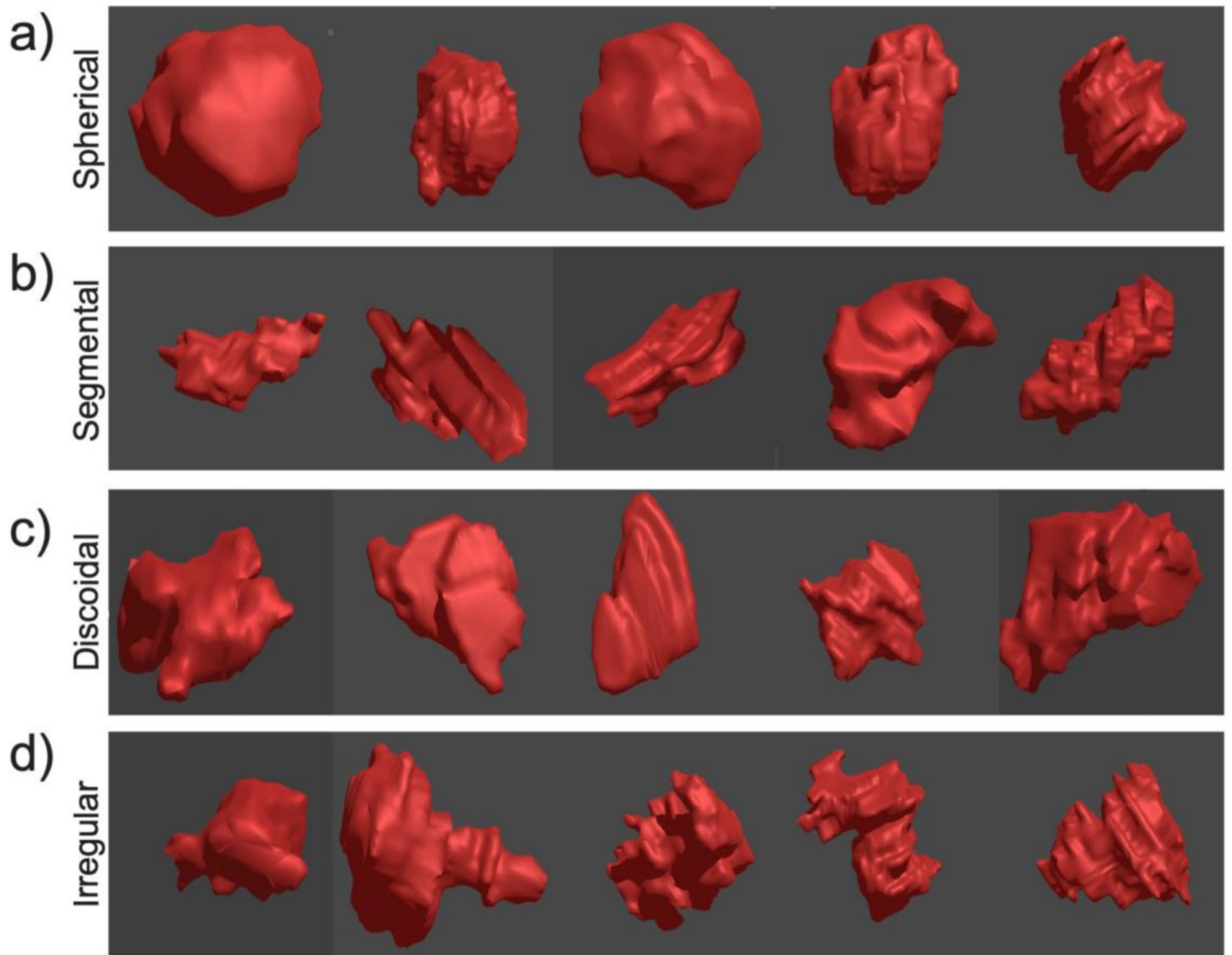


Fig. 2.
Examples of each tumor shape category: spherical (a), segmental (b), discoidal (c), and irregular (d)

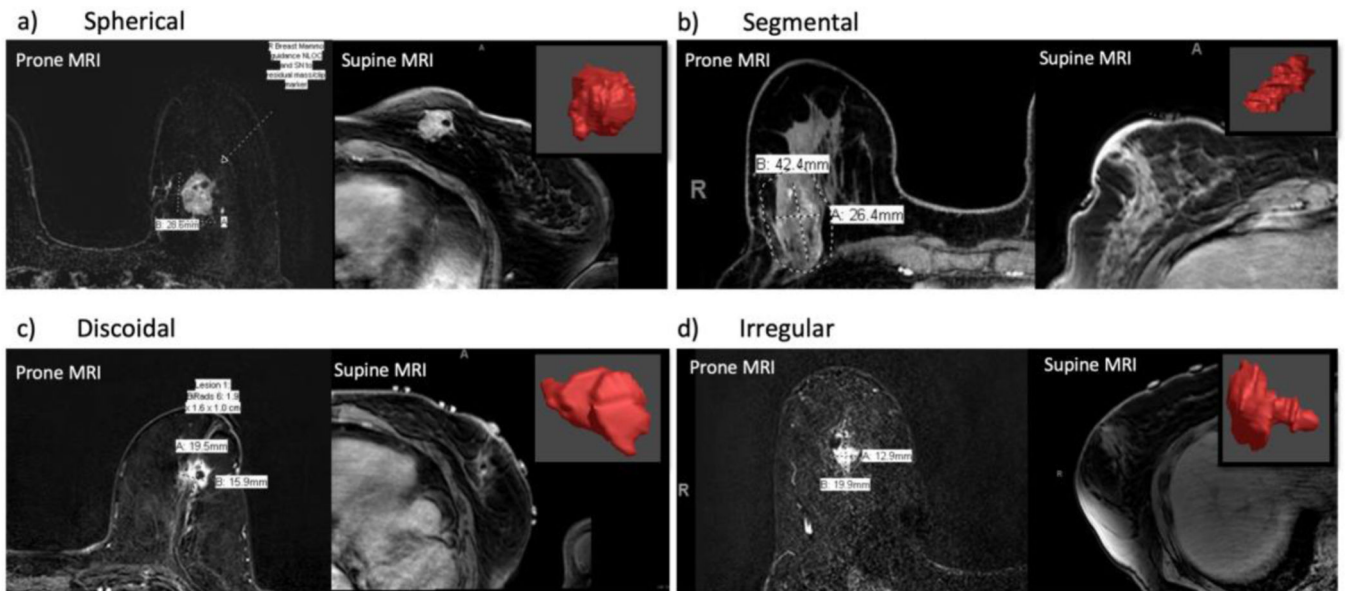


Fig. 3. Segmented shape of categorized tumors compared with prone and supine MRI images. For each of the four tumor shapes there is an example of one patient's prone MRI, supine MRI and 3D tumor model (in red)

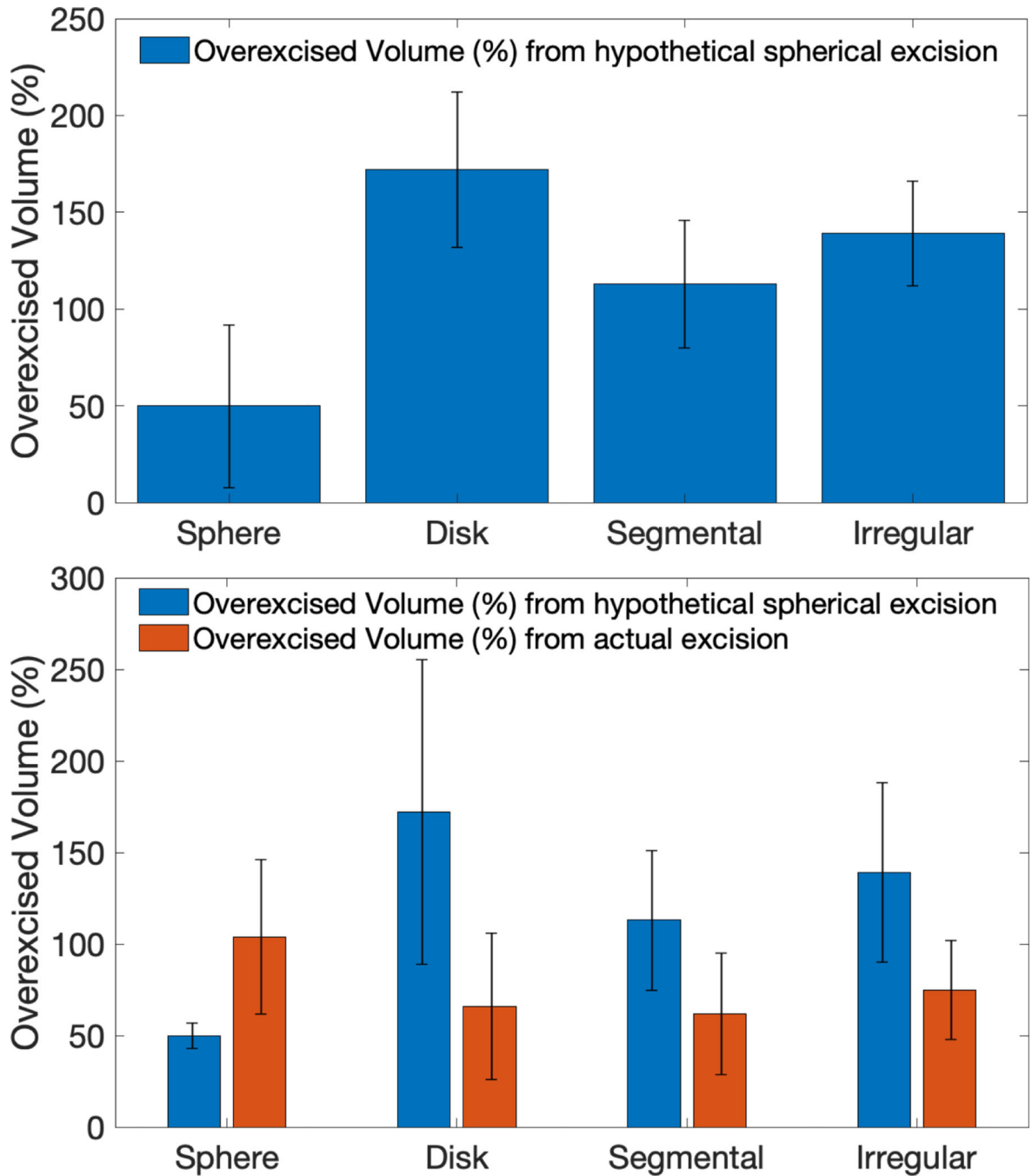


Fig. 4.

(a) Excess volume excised with a spherical excision compared to an ideal excision volume for each shape category (sphere vs. disk, $p < 0.001$; sphere vs. segmental, $p < 0.001$; sphere vs. irregular, $p = 0.003$). (b) Excess volume excised using hypothetical spherical excision vs. actual excess volume excised with supine MRI guided surgery (sphere, $p = 0.05$; disk, $p < 0.001$; segmental, $p = 0.06$; irregular, $p = 0.08$)

Table 1.Frequency of breast cancer shapes¹

Parameter	N	Sphere	Disk	Segmental	Irregular	p
All cases	83	16 (19%)	28 (34%)	24 (29%)	15 (18%)	
DCIS ²	8	0	4 (50%)	4 (50%)	0	0.15
Invasive	75	16 (21%)	24 (32%)	20 (27%)	15 (20%)	
• IDC	64	15 (23%)	20 (31%)	16 (25%)	13 (20%)	0.81
• ILC	11	1 (9%)	4 (36%)	4 (25%)	2 (13%)	

¹Table partially contains data previously published in prior publication materials (Barth, 2019, *Ann Surg Oncol*). Full permission to utilize the previously published dataset was obtained.

²Abbreviations: DCIS, ductal carcinoma in situ ; IDC, invasive ductal carcinoma ; ILC, invasive lobular carcinoma ; ER(+), estrogen receptor positive; HER2(+), human epidermal growth factor receptor 2 positive

Table 2.Associations between tumor and clinical variable and tumor shape¹

Parameter	All cases	Sphere	Disk	Segmental	Irregular	p
Number of patients	83	16	28	24	15	
Patient Age (years)	63.5	62.3	64.7	66.0	58.5	0.08
Pathologic Tumor Diameter (cm)	1.94	1.96	2.03	2.02	1.63	0.80
Maximal Tumor Diameter Prone MRI (cm)	2.45	2.04	2.49	2.65	2.55	0.61
Maximal Tumor Diameter, 3D model (cm)	3.95	2.97	4.65	3.83	3.88	0.002
Avg. Tumor Segmented Volume (cm ³)	8.6	13.6	9.2	7.0	4.5	0.57
ER(+) (%)	75 (90%)	15 (94%)	25 (89%)	21 (88%)	14 (93%)	0.89
HER2(+) (%)	3(4%)	1 (6%)	0(0%)	1 (4%)	1 (7%)	0.62
Positive Nodes (%)	10 (12%)	2 (13%)	4 (14%)	4 (17%)	0 (0%)	0.44
Positive Margin (%)	7 (8%)	2 (13%)	0 (0%)	4 (17%)	1 (7%)	0.17